

## Two-dimensional melting via sine-Gordon duality

Zhengzheng Zhai and Leo Radzihovsky\*

Department of Physics and Center for Theory of Quantum Matter, University of Colorado, Boulder, Colorado 80309, USA



(Received 7 May 2019; revised manuscript received 12 August 2019; published 11 September 2019)

Motivated by the recently developed duality [Pretko and Radzihovsky, *Phys. Rev. Lett.* **120**, 195301 (2018)] between the elasticity of a crystal and a symmetric tensor gauge theory, we explore its classical analog, which is a dual theory of the dislocation-mediated melting of a two-dimensional crystal, formulated in terms of a higher derivative vector sine-Gordon model. It provides a transparent description of the continuous two-stage melting in terms of the renormalization-group relevance of two cosine operators that control the sequential unbinding of dislocations and disclinations, respectively, corresponding to the crystal-to-hexatic and hexatic-to-isotropic fluid transitions. This renormalization-group analysis reproduces the seminal results of the Coulomb gas description, such as the flows of the elastic couplings and of the dislocation and disclination fugacities, as well as the temperature dependence of the associated correlation lengths.

DOI: [10.1103/PhysRevB.100.094105](https://doi.org/10.1103/PhysRevB.100.094105)

### I. INTRODUCTION

#### A. Background and motivation

The theory of continuous two-dimensional (2D) melting, developed by Kosterlitz and Thouless [1], Halperin and Nelson [2], and Young [3] (KTHNY), building on the work of Landau [4], Peierls [5], and Berezinskii [6,7], has become one of the pillars of theoretical physics. Mathematically related to simpler normal-to-superfluid and planar paramagnet-to-ferromagnet transitions in films, described by a 2D  $XY$  model, it is a striking example of the increased importance of thermal fluctuations in low-dimensional systems [8,9]. In contrast to their bulk three-dimensional analogs, where, typically, fluctuations only lead to *quantitative* modifications of mean-field predictions (e.g., values of critical exponents), here the effects are *qualitative* and drastic. Located exactly at the lower-critical dimension, where a local-order-parameter distinction between the high- and low-temperature phases is erased by fluctuations, two-dimensional melting can proceed via a subtle, two-stage, *continuous* transition, driven by the unbinding of topological dislocations and disclination defects. This mechanism, made possible by strong thermal fluctuations, thus provides an alternative route to direct first-order melting, argued by Landau's mean-field analysis [4] to be the *exclusive* scenario.

As such, the continuous two-dimensional melting (and related disordering of a 2D  $XY$  model) is the earliest example of a thermodynamically sharp, *topological* phase transition between two locally disordered phases, which thus does not admit Landau's local order-parameter description. It is controlled by a fixed line, which lends itself to an asymptotically *exact* analysis [1–3].

Although evidence for defects-driven phase transitions has appeared in a number of experiments on liquid crystals [10] and Langmuir-Blodgett films [11], finding simple model

systems that exhibit these phenomena in experiments or simulations has proven to be more challenging. Most studied systems appear to exhibit discontinuous first-order melting that converts a crystal directly into a liquid. However, it appears that two-stage continuous melting has been experimentally observed by Murray [12] and Zahn [13] in beautiful melting experiments on two-dimensional colloids confined between smooth glass plates and superparamagnetic colloidal systems, respectively. In these experiments, an orientationally quasi-long-range ordered but translationally disordered hexatic phase [2] was indeed observed. As was first emphasized by Halperin and Nelson [2], the hexatic liquid, intermediate but thermodynamically distinct from the 2D crystal and the isotropic liquid, is an important signature of the defect-driven two-stage melting. In these two-dimensional colloids, particle positions and the associated topological defects can be directly imaged via digital videomicroscopy, allowing precise quantitative tests of the theory.

#### B. Duality of the two-stage melting transition

The disordering of the simpler 2D  $XY$  model (describing, e.g., a superfluid-normal transition in a film) is well known to admit two complementary descriptions, the 2D Coulomb gas of vortices [14] and its dual sine-Gordon field theory [2,8,15–18]. As with other dualities—a subject with a long history and of much current interest [19]—the sine-Gordon duality has been extensively utilized in a variety of physical contexts. Given that elasticity of a crystal can be thought of as a space-spin coupled vector generalization of an  $XY$  model (with vector phonon Goldstone modes  $u_x, u_y$  replacing the scalar phase angle), it is of interest also to develop an analogous dual sine-Gordon formulation and to use it to study the 2D continuous melting transition.

Indeed, recently, such a complementary description has emerged as a classical limit of the elasticity-to-tensor gauge theory duality [20,21], derived in the context of a new class of topologically ordered fraction matter [22]. As we will detail

\*radzihov@colorado.edu

in the body of the paper, the corresponding dual Hamiltonian is given by

$$\tilde{H} = \int d^2r \left[ \frac{1}{2} \tilde{C}_{ij,kl}^{-1} \partial_i \partial_j \phi \partial_k \partial_l \phi - g_b \sum_{n=1}^p \cos(\mathbf{b}_n \cdot \hat{\mathbf{z}} \times \nabla \phi) - g_s \cos(s_p \phi) \right]. \quad (1)$$

Its key features, which characterize the continuous two-stage melting, are the higher-order ‘‘Laplacian elasticity’’, encoded via elastic constants  $\tilde{C}_{ij,kl}^{-1}$ , and two sine-Gordon types of operators with couplings  $g_b$ ,  $g_s$ , respectively, capturing the importance (fugacities) of dislocation (elementary vector charges  $\mathbf{b}_n$ ) and disclination (elementary scalar charge  $s_p$ ) defects.

To flesh out the essence of this dual description, neglecting inessential details, the above Hamiltonian is schematically described by

$$\tilde{H} \sim \int_{\mathbf{r}} \left[ \frac{1}{2} \tilde{C} (\partial^2 \phi)^2 - g_b \cos(\partial \phi) - g_s \cos(\phi) \right], \quad (2)$$

where  $\int_{\mathbf{r}} \equiv \int d^2r$ . Because of the second-order Laplacian elasticity, standard analysis around the Gaussian fixed line  $g_b = g_s = 0$  shows that the mean-squared fluctuations of Airy-stress potential  $\phi$  diverge quadratically with system size. This leads to an exponentially (as opposed to power-law in a conventional sine-Gordon model) vanishing Debye-Waller factor, and in turn to a strongly irrelevant disclination cosine,  $g_s$ , that can therefore be neglected whenever  $g_b$  is small, i.e., near the Gaussian fixed line.

The schematic Hamiltonian then reduces to

$$\tilde{H}_{\text{cr}} \sim \int_{\mathbf{r}} \left[ \frac{1}{2} \tilde{C} (\partial \chi)^2 - g_b \cos(\chi) \right], \quad (3)$$

with  $\chi = \partial \phi$ . It thus obeys the standard sine-Gordon phenomenology, exhibiting a KT-like ‘‘roughening’’ transition in  $\chi$  with the relevance of  $g_b$ , controlled by the stiffness  $\tilde{C}$  [2,8,15–17]. At small  $\tilde{C} < \tilde{C}_c$ ,  $g_b$  is irrelevant describing the gapless crystal phase with confined dislocations and disclinations. The melting of the crystal is then captured by the relevance of  $g_b$  for  $\tilde{C} > \tilde{C}_c$ , corresponding to a transition into a plasma of unbound dislocations characteristic of a hexatic fluid. Since in this phase  $g_b$  is relevant, at sufficiently long scales the dislocation cosine in Eq. (2) reduces to a harmonic potential for  $\chi$ ,  $-g_b \cos(\partial \phi) \sim \frac{1}{2} g_b (\partial \phi)^2$ . The effective Hamiltonian is then given by

$$\tilde{H}_{\text{hex}} \sim \int_{\mathbf{r}} \left[ \frac{1}{2} g_b (\partial \phi)^2 - g_s \cos(\phi) \right], \quad (4)$$

where we have neglected the  $\tilde{C}$  ‘‘curvature’’ elasticity relative to the gradient one encoded in  $g_b$ , and restored the disclination cosine operator  $g_s \cos(\phi)$ . The resulting conventional sine-Gordon model in  $\phi$  can then exhibit the second KT-like ‘‘roughening’’ transition, capturing the hexatic-to-isotropic fluid transition associated with the unbinding of disclinations. The corresponding RG flow of the dual vector sine-Gordon model is schematically illustrated in Fig. 1. We leave the detailed analysis of this two-stage melting transition to the main body of the paper and the Appendix.

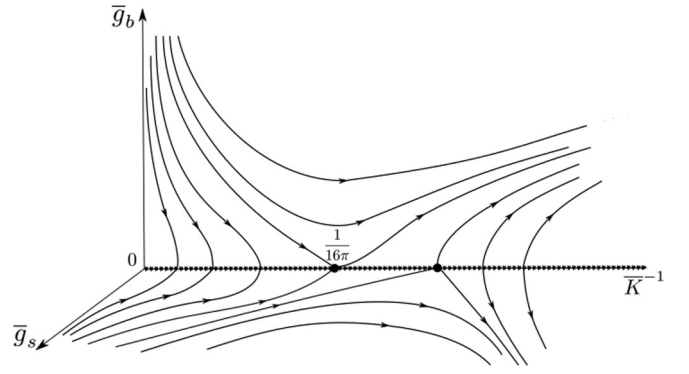


FIG. 1. A schematic illustration of RG flows in the dual vector sine-Gordon model. It describes the two-stage continuous 2D melting, crystal-to-hexatic and hexatic-to-isotropic liquid transitions, associated with consequent relevance of dislocation ( $g_b$ ) and disclination ( $g_s$ ) fugacities, as a function of the elastic modulus  $\bar{K}^{-1} = \frac{2\mu+\lambda}{4a^2\mu(\mu+\lambda)}$ , expressed in terms of the Lamé elastic constants,  $\mu$ ,  $\lambda$  (defined in the main text), and the lattice constant,  $a$ .

### C. Outline

The rest of this paper is organized as follows. In Sec. II, after briefly reviewing the elasticity theory of two-dimensional crystal and its topological defects, we give two detailed complementary derivations of the duality transformation to the vector sine-Gordon model. Utilizing the latter, we straightforwardly reproduce known results for the crystal-hexatic phase transition in Sec. III by focusing on the dislocation fugacity cosine operator and neglecting the irrelevant disclinations. Inside the hexatic phase, we derive a scalar sine-Gordon model for the Airy stress potential that captures the subsequent hexatic-isotropic liquid transition. We conclude in Sec. IV with a summary of our results and a discussion of potential applications of this dual approach.

## II. DUALITY OF 2D MELTING

### A. Two-dimensional elasticity

At low temperatures, the deformations of a crystal do not vary substantially over the atom size, allowing it to be described with a continuum field theory of its phonon Goldstone modes,  $u(\mathbf{r})$ , with a short-distance cutoff set by the lattice spacing  $a$ . The underlying translational symmetry (spontaneously broken by the crystal) requires that the elastic energy is an analytic expansion in the strain field  $\partial_i u_j$ . Due to the underlying rotational symmetry in the target space (i.e., no substrates and/or external fields), the elastic Hamiltonian is further constrained (in harmonic order) to be independent of the antisymmetric part of  $\partial_i u_j$ , i.e., of the local bond angle  $\theta(\mathbf{r}) = \frac{1}{2} \epsilon_{ij} \partial_i u_j = \frac{1}{2} \hat{\mathbf{z}} \cdot \nabla \times \mathbf{u}$ . The elastic Hamiltonian density to harmonic order is thus given by

$$\mathcal{H} = \frac{1}{2} C_{ij,kl} u_{ij} u_{kl}, \quad (5)$$

where  $u_{ij} = \frac{1}{2} (\partial_i \mathbf{r} \cdot \partial_j \mathbf{r} - \delta_{ij})$  is the symmetric nonlinear strain tensor (fully rotationally invariant in the target space), which in the harmonic approximation takes the linear symmetrized form

$$u_{ij} \approx \frac{1}{2} (\partial_i u_j + \partial_j u_i). \quad (6)$$

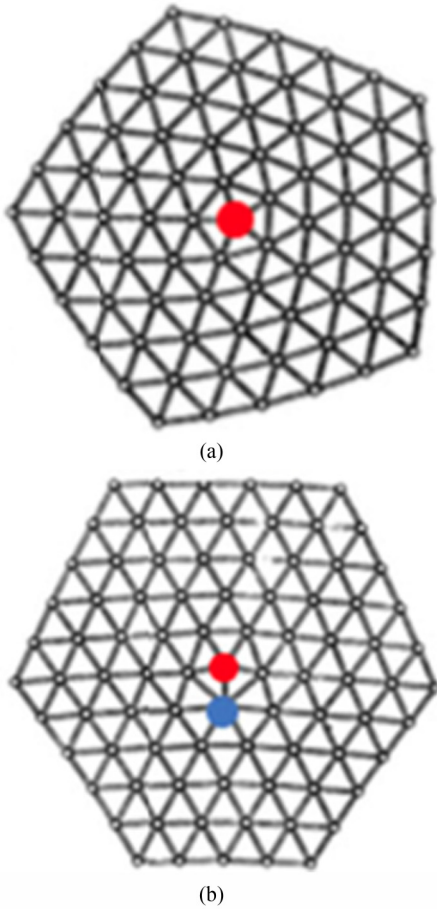


FIG. 2. Topological defects in a 2D hexagonal lattice. (a) A disclination. (b) A dislocation; a dipole of two, opposite charge disclinations. (Figure adapted from Ref. [20].)

$C_{ij,kl}$  is the elastic constant tensor, whose number of independent components is restricted by the symmetry of the crystal. For simplicity, we focus on the isotropic hexagonal lattice, where  $C_{ij,kl}$  takes the form

$$C_{ij,kl} = \lambda \delta_{ij} \delta_{kl} + 2\mu \delta_{ik} \delta_{jl} \quad (7)$$

and is characterized by two independent elastic constants, namely the Lamé coefficients  $\lambda$  and  $\mu$ . As we discuss in Appendix B, an external stress  $\sigma_{ij}^e(\mathbf{r})$  is included through an additional term  $-\sigma_{ij}^e u_{ij}$ , here focusing on the case of a vanishing external stress.

### B. Topological defects

In addition to the single-valued elastic phonon fields, the crystal also exhibits topological defects—disclinations and dislocations—captured by including a non-single-valued part of the phonon distortion field.

Disclinations are topological defects associated with orientational order. A disclination at a point  $\mathbf{r}_0$ , illustrated in Fig. 2(a), is defined by a nonzero closed line-integral of the gradient of the bond angle around  $\mathbf{r}_0$ :

$$\oint_{\mathbf{r}_0} d\theta = \frac{2\pi}{p} s \quad (8)$$

or equivalently in a differential form:

$$\hat{\mathbf{z}} \cdot \nabla \times \nabla \theta = \frac{2\pi}{p} s \delta^2(\mathbf{r} - \mathbf{r}_0) \equiv \frac{2\pi}{p} s(\mathbf{r}), \quad (9)$$

measuring the deficit/surplus bond angle,  $(2\pi/p)s$ , with  $s$  the integer disclination charge in a  $C_p$  symmetric crystal. In the case of a hexagonal lattice,  $p = 6$ . In the above equation,  $s(\mathbf{r})$  is the disclination charge density.

Dislocations are vector topological defects associated with translational order. A dislocation at  $\mathbf{r}_0$  with a Burgers vector-charge  $\mathbf{b}_n$  (that is an elementary lattice vector), as illustrated in Fig. 2(b), is defined by a closed line-integral

$$\oint_{\mathbf{r}_0} d\mathbf{u} = \mathbf{b}_n, \quad (10)$$

or equivalently in the differential form,

$$\hat{\mathbf{z}} \cdot \nabla \times \nabla u_i = b_{i,n} \delta^2(\mathbf{r} - \mathbf{r}_0) \equiv b_i(\mathbf{r}), \quad (11)$$

where  $\mathbf{b}(\mathbf{r})$  is the Burgers charge density. As illustrated in Fig. 2(b), a dislocation is a disclination dipole, and it is therefore energetically less costly than a bare disclination charge.

### C. Vector Coulomb gas formulation

In the presence of topological defects, the distortion field  $\mathbf{u}(\mathbf{r})$  is not single-valued. Along with the associated strain tensor, the distortion field can be decomposed into the single-valued elastic phonon and the singular parts,

$$u_i = \tilde{u}_i + u_i^s, \quad (12)$$

$$u_{ij} = \tilde{u}_{ij} + u_{ij}^s. \quad (13)$$

To include these topological and phonon degrees of freedom, we focus on the partition function (taking  $k_B T = 1$ , i.e., measuring coupling constants in units of thermal energy),

$$Z = \int [d\mathbf{u}] e^{-\int_r \mathcal{H}[\mathbf{u}]} = \int [d\tilde{\mathbf{u}}][d\mathbf{u}^s] \int [d\sigma_{ij}(\mathbf{r})] e^{-\int_r \mathcal{H}[\mathbf{u}, \sigma_{ij}]}, \quad (14)$$

where the trace over  $\mathbf{u}(\mathbf{r})$  implicitly includes both phonons and topological defects by allowing non-single-valued distortions. In the second form above, we decoupled the elastic energy by introducing a Hubbard-Stratonovich tensor field—the *symmetric* stress tensor  $\sigma_{ij}(\mathbf{r})$  [17], with the resulting Hamiltonian density given by

$$\begin{aligned} \mathcal{H}[\mathbf{u}, \sigma_{ij}] &= \frac{1}{2} C_{ij,kl}^{-1} \sigma_{ij} \sigma_{kl} + i \sigma_{ij} u_{ij} \\ &= \frac{1}{2} C_{ij,kl}^{-1} \sigma_{ij} \sigma_{kl} + i \sigma_{ij} (\partial_i \tilde{u}_j + u_{ij}^s). \end{aligned} \quad (15)$$

Above, for a 2D hexagonal lattice,

$$C_{ij,kl}^{-1} = -\frac{\lambda}{4\mu(\mu + \lambda)} \delta_{ij} \delta_{kl} + \frac{1}{2\mu} \delta_{ik} \delta_{jl}. \quad (16)$$

Tracing over the single-valued phonons  $\tilde{\mathbf{u}}$  enforces the divergenceless stress constraint [via the  $\delta$ -function identity  $\frac{1}{2\pi} \int_{-\infty}^{\infty} du e^{iuf} = \delta(f)$ ]

$$\partial_i \sigma_{ij} = 0, \quad (17)$$

solved with a scalar Airy stress potential,  $\phi(\mathbf{r})$ ,

$$\sigma_{ij} = \epsilon_{ik} \epsilon_{jl} \partial_k \partial_l \phi. \quad (18)$$

Expressing the Hamiltonian density in terms of  $\phi(\mathbf{r})$ , and integrating by parts in the second linear term, we utilize the defects conditions, Eqs. (9) and (11),

$$\epsilon_{ik}\epsilon_{jl}\partial_l\partial_k u_{ij}^s = \epsilon_{ik}\epsilon_{jl}\partial_l\partial_k(\partial_i u_j^s - \epsilon_{ij}\theta^s), \quad (19a)$$

$$= \epsilon_{ki}\partial_k b_i(\mathbf{r}) + \epsilon_{ki}\partial_k \partial_i \theta(\mathbf{r}), \quad (19b)$$

$$= \hat{\mathbf{z}} \cdot \nabla \times \mathbf{b} + \frac{2\pi}{6} s(\mathbf{r}), \quad (19c)$$

to obtain

$$\mathcal{H}[\phi] = \frac{1}{2} \tilde{C}_{ij,kl}^{-1} \partial_i \partial_j \phi \partial_k \partial_l \phi + i\phi \left( \frac{2\pi}{6} s + \hat{\mathbf{z}} \cdot \nabla \times \mathbf{b} \right). \quad (20)$$

In the above,  $\tilde{C}_{ij,kl}^{-1} = \epsilon_{ia}\epsilon_{jb}\epsilon_{kc}\epsilon_{ld} C_{ab,cd}^{-1}$ .

Focusing on dislocations and neglecting the high-energy disclination defects, we can straightforwardly integrate out  $\phi(\mathbf{r})$  in the partition function, obtaining a dislocations vector Coulomb gas Hamiltonian

$$H_b = \frac{1}{2} \int \frac{d^2 q}{(2\pi)^2} b_i(\mathbf{q}) \tilde{K}_{ij}(\mathbf{q}) b_j(-\mathbf{q}), \quad (21)$$

where the tensor Coulomb interaction in Fourier and coordinate spaces is given by

$$\tilde{K}_{ij}(\mathbf{q}) = \frac{K}{q^2} \left( \delta_{ij} - \frac{q_i q_j}{q^2} \right), \quad (22)$$

$$K_{ij}(\mathbf{r}) = -\frac{K}{4\pi} \left( \delta_{ij} \ln(r/a) - \frac{r_i r_j}{r^2} \right), \quad (23)$$

with  $K = \frac{4\mu(\mu+\lambda)}{2\mu+\lambda}$ .

Thus, the dislocations vector Coulomb gas Hamiltonian in real space reduces to

$$H_b = -\frac{K}{8\pi} \int_{\mathbf{r}_1, \mathbf{r}_2} \left[ \mathbf{b}(\mathbf{r}_1) \cdot \mathbf{b}(\mathbf{r}_2) \ln \frac{|\mathbf{r}_1 - \mathbf{r}_2|}{a} - \frac{\mathbf{b}(\mathbf{r}_1) \cdot (\mathbf{r}_1 - \mathbf{r}_2)(\mathbf{r}_1 - \mathbf{r}_2) \cdot \mathbf{b}(\mathbf{r}_2)}{|\mathbf{r}_1 - \mathbf{r}_2|^2} \right], \quad (24)$$

which, in the discrete form and supplemented with core energies (see below), is exactly the vector Coulomb gas model

used by Nelson and Halperin [2] and by Young [3] in the theory of 2D continuous two-stage melting.

#### D. Dual vector sine-Gordon model

Motivated by the sine-Gordon description of the XY model, we dualize the elasticity by transforming the above vector Coulomb gas into a vector sine-Gordon model, and reexamine the two-stage continuous 2D melting transition from this complementary approach.

Dislocation and disclination densities on a hexagonal lattice are given as a sum of their discrete charges,

$$\mathbf{b}(\mathbf{r}) = \sum_{\mathbf{r}_n} \mathbf{b}_{\mathbf{r}_n} \delta^2(\mathbf{r} - \mathbf{r}_n), \quad (25)$$

$$s(\mathbf{r}) = \sum_{\mathbf{r}_n} s_{\mathbf{r}_n} \delta^2(\mathbf{r} - \mathbf{r}_n), \quad (26)$$

where  $\mathbf{r}_n = a(n_1 \hat{\mathbf{e}}_1 + n_2 \hat{\mathbf{e}}_2)$  ( $n_1, n_2 \in \mathbb{Z}$ ) are triangular lattice vectors spanned by unit vectors  $\hat{\mathbf{e}}_1 = \hat{\mathbf{x}}$  and  $\hat{\mathbf{e}}_2 = \frac{1}{2}\hat{\mathbf{x}} + \frac{\sqrt{3}}{2}\hat{\mathbf{y}}$ , and  $\mathbf{b}_{\mathbf{r}_n} = a(n_1 \hat{\mathbf{e}}_1 + n_2 \hat{\mathbf{e}}_2)$  and  $s_{\mathbf{r}_n} \in \mathbb{Z}$  are dislocation and disclination charges, respectively.

In terms of these discrete topological defect charges, the Hamiltonian is given by

$$H = \frac{1}{2} \int_{\mathbf{r}} \tilde{C}_{ij,kl}^{-1} \partial_i \partial_j \phi \partial_k \partial_l \phi + \sum_{\mathbf{r}_n} [\tilde{E}_b \mathbf{b}_{\mathbf{r}_n}^2 + E_s s_{\mathbf{r}_n}^2] + \sum_{\mathbf{r}_n} \left[ i \frac{2\pi}{6} \phi(\mathbf{r}_n) s_{\mathbf{r}_n} - i \hat{\mathbf{z}} \times \nabla \phi(\mathbf{r}_n) \cdot \mathbf{b}_{\mathbf{r}_n} \right], \quad (27)$$

where we have added dislocation and disclination core energies  $E_b = a^2 \tilde{E}_b$  and  $E_s$  to account for the defects' energetics at the scales of the lattice constant, not accounted for by the elasticity theory [2]. The partition function involves an integration over potential  $\phi(\mathbf{r}_n)$  and summation over the dislocation and disclination charges. Following a standard analysis [1,2,14,15,17],

$$\begin{aligned} Z &= \int [d\phi] \sum_{\{s_{\mathbf{r}_n}\}} \sum_{\{\mathbf{b}_{\mathbf{r}_n}\}} \prod_{\mathbf{r}_n} e^{-H[\phi, \mathbf{b}_{\mathbf{r}_n}, s_{\mathbf{r}_n}]} = \int [d\phi] e^{-\frac{1}{2} \int_{\mathbf{r}} \tilde{C}_{ij,kl}^{-1} \partial_i \partial_j \phi \partial_k \partial_l \phi} \sum_{\{s_{\mathbf{r}_n}\}} \sum_{\{\mathbf{b}_{\mathbf{r}_n}\}} \prod_{\mathbf{r}_n} [e^{-i \frac{2\pi}{6} \phi(\mathbf{r}_n) s_{\mathbf{r}_n} - E_s s_{\mathbf{r}_n}^2} e^{i \hat{\mathbf{z}} \times \nabla \phi(\mathbf{r}_n) \cdot \mathbf{b}_{\mathbf{r}_n} - \tilde{E}_b \mathbf{b}_{\mathbf{r}_n}^2}] \\ &= \int [d\phi] e^{-\frac{1}{2} \int_{\mathbf{r}} \tilde{C}_{ij,kl}^{-1} \partial_i \partial_j \phi \partial_k \partial_l \phi} \left[ 1 + e^{-2E_s} \int \frac{d^2 r_1}{a^2} \frac{d^2 r_2}{a^2} e^{-i \frac{2\pi}{6} \phi(\mathbf{r}_1)} e^{i \frac{2\pi}{6} \phi(\mathbf{r}_2)} + \dots \right] \\ &\quad \times \left[ 1 + e^{-2E_b} \sum_{n=1}^3 \int \frac{d^2 r_1}{a^2} \frac{d^2 r_2}{a^2} e^{-i \hat{\mathbf{z}} \times \nabla \phi(\mathbf{r}_1) \cdot \mathbf{b}_n} e^{i \hat{\mathbf{z}} \times \nabla \phi(\mathbf{r}_2) \cdot \mathbf{b}_n} + \dots \right], \\ &= \int [d\phi] e^{-\frac{1}{2} \int_{\mathbf{r}} \tilde{C}_{ij,kl}^{-1} \partial_i \partial_j \phi \partial_k \partial_l \phi} \left[ 1 + e^{-E_s} \int \frac{d^2 r_1}{a^2} (e^{i \frac{2\pi}{6} \phi(\mathbf{r}_1)} + e^{-i \frac{2\pi}{6} \phi(\mathbf{r}_1)}) \right. \\ &\quad \left. + \frac{1}{2!} e^{-2E_s} \int \frac{d^2 r_1}{a^2} \frac{d^2 r_2}{a^2} (e^{i \frac{2\pi}{6} \phi(\mathbf{r}_1)} + e^{-i \frac{2\pi}{6} \phi(\mathbf{r}_1)}) (e^{i \frac{2\pi}{6} \phi(\mathbf{r}_2)} + e^{-i \frac{2\pi}{6} \phi(\mathbf{r}_2)}) + \dots \right] \\ &\quad \times \prod_{n=1,2,3} \left[ 1 + e^{-E_b} \int \frac{d^2 r_1}{a^2} (e^{i \hat{\mathbf{z}} \times \nabla \phi(\mathbf{r}_1) \cdot \mathbf{b}_n} + e^{-i \hat{\mathbf{z}} \times \nabla \phi(\mathbf{r}_1) \cdot \mathbf{b}_n}) \right] \end{aligned}$$



$$\begin{aligned}
& + \frac{1}{2!} e^{-2E_b} \int \frac{d^2 r_1}{a^2} \frac{d^2 r_2}{a^2} (e^{i\hat{\mathbf{z}} \times \nabla \phi(\mathbf{r}_1) \cdot \mathbf{b}_n} + e^{-i\hat{\mathbf{z}} \times \nabla \phi(\mathbf{r}_1) \cdot \mathbf{b}_n}) (e^{i\hat{\mathbf{z}} \times \nabla \phi(\mathbf{r}_2) \cdot \mathbf{b}_n} + e^{-i\hat{\mathbf{z}} \times \nabla \phi(\mathbf{r}_2) \cdot \mathbf{b}_n}) + \dots \Big] \\
& \equiv \int [d\phi] e^{-\tilde{H}}, \tag{28}
\end{aligned}$$

where non-neutral charge configurations vanish automatically after integration over  $\phi(\mathbf{r})$ . In the last step above, we have summed over only the positive/negative single charges of dislocation and disclination, and we obtain the dual vector sine-Gordon Hamiltonian,

$$\begin{aligned}
\tilde{H} = \int_{\mathbf{r}} \Big[ & \frac{1}{2} \tilde{C}_{ij,kl}^{-1} \partial_i \partial_j \phi \partial_k \partial_l \phi - g_b \sum_{n=1}^3 \cos(\mathbf{b}_n \cdot \hat{\mathbf{z}} \times \nabla \phi) \\
& - g_s \cos\left(\frac{2\pi}{6} \phi\right) \Big]. \tag{29}
\end{aligned}$$

In the above equation, the couplings  $g_b = \frac{2}{a^2} e^{-E_b}$ ,  $g_s = \frac{2}{a^2} e^{-E_s}$  are proportional to dislocation and disclination fugacities, and the three elementary dislocation Burgers vectors are given by  $\mathbf{b}_1 = a\hat{\mathbf{x}}$ ,  $\mathbf{b}_2 = -\frac{a}{2}\hat{\mathbf{x}} + \frac{a\sqrt{3}}{2}\hat{\mathbf{y}}$ ,  $\mathbf{b}_3 = -\mathbf{b}_1 - \mathbf{b}_2 = -\frac{a}{2}\hat{\mathbf{x}} - \frac{a\sqrt{3}}{2}\hat{\mathbf{y}}$ .

### E. Vector sine-Gordon duality redux

The above derivation of the dual vector sine-Gordon model departed from the conventional phonon-only elastic model of a 2D crystal, Eq. (5). As discussed in Sec. II B, target space rotational invariance of the crystal is incorporated by building the theory based on the *symmetric* tensor part  $u_{ij}$ , Eq. (6), of the full strain tensor,  $\partial_i u_j$ , i.e., forbidding an explicit dependence on the local bond angle  $\theta = \frac{1}{2} \epsilon_{ij} \partial_i u_j$ , which corresponds to an angle of rotation of the crystal.

Alternatively, the rotational invariance of a crystal can be formulated as a gaugelike (minimal) coupling between the full strain tensor  $\partial_i u_j$  and the bond angle  $\theta(\mathbf{r})$ , encoded in the Hamiltonian density

$$\mathcal{H} = \frac{1}{2} C_{ij,kl} (\partial_i u_j - \theta \epsilon_{ij}) (\partial_k u_l - \theta \epsilon_{kl}) + \frac{1}{2} K (\partial_i \theta)^2. \tag{30}$$

It can be straightforwardly verified that an integration over the bond-angle field  $\theta$  ‘‘Higgses out’’ [17,18] the antisymmetric component of the strain tensor at long wavelengths recovering the conventional elastic Hamiltonian in (5).

We now decouple the strain and bond elastic terms by introducing two Hubbard-Stratonovich fields—the stress field  $\sigma_{ij}$  and the torque ‘‘current’’  $j_i$ ,

$$\begin{aligned}
\mathcal{H}[\mathbf{u}, \theta; \sigma_{ij}, j_i] = & \frac{1}{2} C_{ij,kl}^{-1} \sigma_{ij} \sigma_{kl} + i \sigma_{ij} (\partial_i u_j - \theta \epsilon_{ij}) \\
& + \frac{1}{2} K^{-1} j_i^2 + i j_i \partial_i \theta. \tag{31}
\end{aligned}$$

We note that because  $\partial_i u_j$  is not symmetrized, the stress tensor  $\sigma_{ij}$  is not symmetric here. In the presence of topological defects, we again decompose the distortion field  $\mathbf{u}$  and the bond angle  $\theta$  into the smooth elastic and non-single-valued components,

$$u_i = \tilde{u}_i + u_i^s, \quad \theta = \tilde{\theta} + \theta^s, \tag{32}$$

which allow for dislocation and disclination defects, respectively.

Integrating out the single-valued parts  $\tilde{\mathbf{u}}$  and  $\tilde{\theta}$  enforces two constraints,

$$\partial_i \sigma_{ij} = 0, \tag{33a}$$

$$\partial_i j_i + \epsilon_{ij} \sigma_{ij} = 0. \tag{33b}$$

The first one is solved via a vector gauge field  $\mathbf{A}$  with

$$\sigma_{ij} = \epsilon_{ik} \partial_k A_j, \tag{34}$$

which transforms the second constraint into

$$\partial_i (j_i + A_i) = 0. \tag{35}$$

It is then solved by introducing another scalar potential  $\phi$  via  $j_i = \epsilon_{ik} \partial_k \phi - A_i$ . Expressing the Hamiltonian (31) in terms of gauge potentials,  $\mathbf{A}(\mathbf{r})$  and  $\phi(\mathbf{r})$ , integrating by parts, and using the definitions of dislocation  $\mathbf{b}(\mathbf{r})$  and disclination  $s(\mathbf{r})$  densities, the Hamiltonian density takes the form

$$\begin{aligned}
\mathcal{H} = & \frac{1}{2} C_{ij,kl}^{-1} \epsilon_{im} \epsilon_{kn} \partial_m A_j \partial_n A_l + \frac{1}{2} K^{-1} (\epsilon_{ik} \partial_k \phi - A_i)^2 \\
& + i A_i b_i + i \phi \frac{2\pi}{p} s. \tag{36}
\end{aligned}$$

This model is evidently gauge-covariant under a local transformation,

$$\mathbf{A}(\mathbf{r}) \rightarrow \mathbf{A}(\mathbf{r}) + \hat{\mathbf{z}} \times \nabla \alpha(\mathbf{r}), \tag{37a}$$

$$\phi(\mathbf{r}) \rightarrow \phi(\mathbf{r}) + \alpha(\mathbf{r}). \tag{37b}$$

Integrating over the vector potential  $\mathbf{A}(\mathbf{r})$  in the partition function to lowest order yields

$$A_i = \epsilon_{ik} \partial_k \phi \tag{38}$$

(an effective Higgs mechanism [17,18]) and allows us to eliminate  $\mathbf{A}(\mathbf{r})$  in favor of  $\phi(\mathbf{r})$  and to give the effective Hamiltonian density

$$\mathcal{H}[\phi] = \frac{1}{2} \tilde{C}_{ij,kl}^{-1} \partial_i \partial_j \phi \partial_k \partial_l \phi + i \phi \left( \frac{2\pi}{p} s + \hat{\mathbf{z}} \cdot \nabla \times \mathbf{b} \right), \tag{39}$$

which is identical to that found in (20), which, when supplemented by dislocation and disclination core energies and summed over the defects, gives the dual vector sine-Gordon model, Eq. (29).

### F. Energetics of defects

Inside the crystal state, the background defect density vanishes. In terms of the dual defects model, (20) and (39), we can simply set the defect charges to zero,  $s = \mathbf{b} = 0$ . In terms of the generalized sine-Gordon model, (29), this corresponds

to the irrelevance of both cosines, i.e., vanishing couplings,  $g_s = g_b = 0$ ,

$$H_{\text{cr}} = \frac{1}{2} \int_{\mathbf{r}} \tilde{C}_{ij,kl}^{-1} \partial_i \partial_j \phi \partial_k \partial_l \phi, \quad (40a)$$

$$= \frac{1}{2} K^{-1} \int_{\mathbf{r}} (\nabla^2 \phi)^2, \quad (40b)$$

where  $\tilde{C}_{ij,kl}^{-1} = \epsilon_{ia} \epsilon_{jb} \epsilon_{kc} \epsilon_{ld} C_{ab,cd}^{-1}$ , and we have specialized it to that of a hexagonal lattice, obtaining (40b) with  $K^{-1} = \frac{2\mu+\lambda}{4\mu(\mu+\lambda)}$ .

The energy of a single disclination can be obtained by taking  $s(\mathbf{r}) = 2\pi \delta^2(\mathbf{r})$ . Solving the corresponding Euler-Lagrange equation for  $\phi$  gives

$$\phi_s^{\text{cr}}(\mathbf{k}) = \frac{i2\pi K}{k^4}, \quad (41)$$

which for the energy of a single disclination in a crystal state gives a well-known result,

$$E_s^{\text{cr}} = \frac{1}{2} K^{-1} \int d^2r (\nabla^2 \phi_s)^2, \quad (42a)$$

$$= \frac{1}{2} K \int_{L^{-1}} d^2k \frac{1}{k^4} \sim KL^2, \quad (42b)$$

where  $L$  is the linear extent of the crystal.

Similarly, for a single dislocation, such as  $\mathbf{b}(\mathbf{r}) = \mathbf{b}_1 \delta^2(\mathbf{r}) = a \hat{\mathbf{x}} \delta^2(\mathbf{r})$ , the corresponding Euler-Lagrange equation for  $\phi$  gives

$$\phi_b^{\text{cr}}(\mathbf{k}) = \frac{aKk_y}{k^4} = \frac{aK \sin \theta}{k^3}, \quad (43)$$

where  $\theta$  is the angle between the direction of  $\mathbf{k}$  and the  $\hat{\mathbf{x}}$  axis. Therefore, the energy of a single dislocation in the crystal state is

$$E_b^{\text{cr}} = \frac{1}{2} K^{-1} \int d^2r (\nabla^2 \phi_b^{\text{cr}})^2, \quad (44a)$$

$$= \frac{1}{2} Ka^2 \int_{L^{-1}} \frac{d^2k}{(2\pi)^2} \frac{\sin^2 \theta}{k^2}, \quad (44b)$$

$$= \frac{1}{8} Ka^2 \ln \frac{L}{a} \sim K \ln L. \quad (44c)$$

The  $C_3$  rotational symmetry guarantees that the energies for the other single dislocations,  $\mathbf{b}(\mathbf{r}) = \mathbf{b}_2 \delta^2(\mathbf{r})$  and  $\mathbf{b}(\mathbf{r}) = \mathbf{b}_3 \delta^2(\mathbf{r})$ , are identical.

### III. RENORMALIZATION-GROUP ANALYSIS OF THE MELTING TRANSITION

As discussed in the Introduction, and calculated above, within the crystal state with a vanishing background defect density the energy of a single dislocation scales as  $E_b \sim \ln L$ , while the energy of a single disclination scales as  $E_s \sim L^2$ , where  $L$  is the linear extent of the crystal. Thus, as discovered by Nelson and Halperin [2], above the critical melting temperature  $T_m$  the dislocations will unbind first while the disclinations remain confined, leading to the orientationally ordered hexatic liquid, which is stable in a finite-temperature range  $T_m < T < T_{\text{hex}}$ .

More formally, within the dual sine-Gordon model, this is reflected by the irrelevance of the disclination cosine operator at the Gaussian fixed line. Computing its average in a system of size  $L$ , we indeed find

$$\left\langle \int d^2r \cos\left(\frac{2\pi}{6}\phi\right) \right\rangle = \int d^2r e^{-\frac{\pi^2}{18} \langle \phi^2(\mathbf{r}) \rangle} \quad (45a)$$

$$= \int d^2r e^{-\frac{\pi^2}{18} KL^2} \quad (45b)$$

$$\sim L^2 e^{-L^2} \rightarrow 0. \quad (45c)$$

This analysis [that can be more formally elevated to a renormalization-group (RG) computation] demonstrates that the disclination cosine operator,  $g_s$ , is strongly irrelevant around the Gaussian fixed line, i.e., when the dislocation cosine,  $g_b$ , is small, corresponding to the absence of screening of disclinations by dislocations.

#### A. Crystal-hexatic melting transition

Thus, within the crystal and near the crystal-to-hexatic transition, we can neglect the disclination cosine, setting  $g_s = 0$ , reducing the effective Hamiltonian to

$$\tilde{H}_{\text{cr}} = \int_{\mathbf{r}} \left[ \frac{1}{2} \tilde{C}_{ij,kl}^{-1} \partial_i \partial_j \phi \partial_k \partial_l \phi - g_b \sum_{n=1}^3 \cos(\mathbf{b}_n \cdot \hat{\mathbf{z}} \times \nabla \phi) \right]. \quad (46)$$

The RG analysis of this model is more convenient in an equivalent description in terms of a divergenceless vector field  $\mathbf{A} = \hat{\mathbf{z}} \times \nabla \phi$ ,

$$\tilde{H}_{\text{cr}} = \int_{\mathbf{r}} \left[ \frac{1}{2} C_{ij,kl}^{-1} \epsilon_{im} \epsilon_{kn} \partial_m A_j \partial_n A_l + \frac{\alpha}{2} (\nabla \cdot \mathbf{A})^2 - g_b \sum_{n=1}^3 \cos(\mathbf{b}_n \cdot \mathbf{A}) \right], \quad (47)$$

with the constraint  $\nabla \cdot \mathbf{A} = \mathbf{0}$  imposed energetically via a ‘‘mass’’ term  $\frac{\alpha}{2} (\nabla \cdot \mathbf{A})^2$  added to the Hamiltonian, with  $\alpha \rightarrow \infty$  taken at the end of the calculation. Interestingly, our model is mathematically closely related to that for the roughening transition of a crystal pinned by a commensurate substrate, studied by Ohta [23] and by Levin and Dawson [24].

Specializing  $C_{ij,kl}^{-1}$  to a hexagonal lattice, Eq. (16), the Hamiltonian reduces to

$$\tilde{H}_{\text{cr}} = \int_{\mathbf{r}} \left[ \frac{K^{-1}}{2} (\partial_i A_j)^2 + \frac{B}{2} \partial_i A_j \partial_j A_i + \frac{\alpha}{2} (\nabla \cdot \mathbf{A})^2 - g_b \sum_{n=1}^3 \cos(\mathbf{b}_n \cdot \mathbf{A}) \right], \quad (48)$$

where the couplings are

$$K^{-1} = \frac{2\mu + \lambda}{4\mu(\mu + \lambda)}, \quad (49a)$$

$$B = \frac{\lambda}{4\mu(\mu + \lambda)}. \quad (49b)$$

In the physical limit  $\alpha \rightarrow \infty$ , the dislocation-free, Gaussian propagator is given by

$$\langle A_i(\mathbf{q})A_j(\mathbf{q}') \rangle_0 = \frac{K}{q^2} P_{ij}^T(\mathbf{q})(2\pi)^2 \delta^2(\mathbf{q} + \mathbf{q}'), \quad (50)$$

a purely transverse form, with the transverse projection operator,  $P_{ij}^T(\mathbf{q}) = \delta_{ij} - \frac{q_i q_j}{q^2}$ , consistent with (23), encoding the target-space rotational invariance of the crystal [2,3].

To describe the melting transition, we need to include dislocations encoded in the  $g_b$  cosine operator. Although at low temperature (corresponding to large elastic constants and small  $K^{-1}$ ) a perturbative expansion in  $g_b$  is convergent (i.e., the fixed line  $g_b = g_s = 0$  is stable), it breaks down for  $K$  below a critical value, indicating an entropic proliferation of large dislocation pairs for  $T > T_m$ .

To treat this high-temperature nonperturbative regime requires an RG analysis. Relegating the details to Appendix A, here we present the highlights of the analysis and its results. To control the divergent perturbation theory, we employ the momentum-shell coarse-graining RG by decomposing the vector field  $\mathbf{A}(\mathbf{r})$  into its short-scale and long-scale modes,  $A_i(\mathbf{r}) = A_i^<(\mathbf{r}) + A_i^>(\mathbf{r})$ , with

$$A_i^<(\mathbf{r}) = \int_{0 < q < \Lambda/b} \frac{d^2 q}{(2\pi)^2} e^{i\mathbf{q}\cdot\mathbf{r}} A_i(\mathbf{q}), \quad (51a)$$

$$A_i^>(\mathbf{r}) = \int_{\Lambda/b < q < \Lambda} \frac{d^2 q}{(2\pi)^2} e^{i\mathbf{q}\cdot\mathbf{r}} A_i(\mathbf{q}), \quad (51b)$$

where the ultraviolet cutoff  $\Lambda = 2\pi/a$ , and the rescaling factor  $b > 1$  defines the width of the momentum shell,  $\Lambda/b < q < \Lambda$ . Following a standard analysis, we integrate short-scale modes  $A_i^>(\mathbf{r})$  out of the partition function, obtaining a coarse-grained Hamiltonian for the long-scale modes,  $A_i^<(\mathbf{r})$ , with the renormalized coupling  $K_R^{-1}(b)$ ,  $B_R(b)$ , and  $g_{bR}(b)$  satisfying

$$K_R^{-1}(b) = K^{-1} + J_2 g_b^2, \quad (52a)$$

$$B_R(b) = B + J_3 g_b^2, \quad (52b)$$

$$g_{bR}(b) = g_b e^{-\frac{1}{2} G_m^>(0)} + J_1 g_b^2, \quad (52c)$$

valid to second-order in  $g_b$ . The Green's function appearing above is given by

$$G_{nm}^>(\mathbf{r}_1 - \mathbf{r}_2) \equiv b_i^n b_j^m \langle A_i^>(\mathbf{r}_1) A_j^>(\mathbf{r}_2) \rangle_0^>, \quad (53)$$

and  $J_i$  factors are defined as

$$J_1 = \pi a^2 \left[ e^{\frac{\bar{K}}{16\pi}} I_0\left(\frac{\bar{K}}{8\pi}\right) + \left(\frac{\bar{K}}{16\pi} - 1\right) \right] \ln b, \quad (54a)$$

$$J_2 = \frac{\pi a^6}{4} \left\{ e^{\frac{\bar{K}}{8\pi}} \left[ \frac{3}{2} I_0\left(\frac{\bar{K}}{8\pi}\right) - \frac{3}{4} I_1\left(\frac{\bar{K}}{8\pi}\right) \right] + \frac{3}{2} \left( \frac{\bar{K}}{16\pi} - 1 \right) \right\} \ln b, \quad (54b)$$

$$J_3 = \frac{3\pi a^6}{16} e^{\frac{\bar{K}}{8\pi}} I_1\left(\frac{\bar{K}}{8\pi}\right) \ln b, \quad (54c)$$

where  $I_0(x)$  and  $I_1(x)$  are modified Bessel functions.

It is convenient to examine an infinitesimal form of these RG equations by taking  $b = e^{\delta l}$  with  $\delta l \ll 1$ . Near the melting critical point  $K_R^{-1}(l \rightarrow \infty) \equiv K_{R*}^{-1} = \frac{a^2}{16\pi}$ ,  $g_{bR}(l \rightarrow \infty) \equiv g_b^* = 0$ , this then gives RG differential flow equations for the dimensionless coupling constants  $\bar{K}^{-1}(l) = K^{-1}/a^2$ ,  $\bar{B}(l) = B/a^2$ , and  $\bar{g}_b(l) = g_b a^2$ ,

$$\frac{d\bar{K}^{-1}(l)}{dl} = \frac{3\pi}{8} \left[ e^2 \left( I_0(2) - \frac{1}{2} I_1(2) \right) \right] \bar{g}_b^2(l), \quad (55a)$$

$$\frac{d\bar{B}(l)}{dl} = \frac{3\pi}{16} e^2 I_1(2) \bar{g}_b^2(l), \quad (55b)$$

$$\frac{d\bar{g}_b(l)}{dl} = \left( 2 - \frac{\bar{K}}{8\pi} \right) \bar{g}_b + \pi e I_0(2) \bar{g}_b^2(l). \quad (55c)$$

Using the definitions in terms of the dimensionless Lamé elastic constants  $\bar{\mu} = \mu a^2$ ,  $\bar{\lambda} = \lambda a^2$ , and the fugacity  $y$ ,

$$\bar{K}^{-1} = \frac{1}{4} \left( \frac{1}{\bar{\mu}} + \frac{1}{\bar{\mu} + \bar{\lambda}} \right), \quad (56a)$$

$$\bar{B} = \frac{1}{4} \left( \frac{1}{\bar{\mu}} - \frac{1}{\bar{\mu} + \bar{\lambda}} \right), \quad (56b)$$

$$\bar{g}_b = 2e^{-E_b} = 2y, \quad (56c)$$

our equations reduce exactly to the seminal RG flows for the inverse shear modulus,  $\bar{\mu}^{-1}(l)$ , the inverse bulk modulus  $[\bar{\mu}(l) + \bar{\lambda}(l)]^{-1}$ , and the effective fugacity  $y(l)$ , respectively,

$$\frac{d\bar{\mu}^{-1}}{dl} = 3\pi e^2 I_0(2) y^2, \quad (57a)$$

$$\frac{d(\bar{\mu} + \bar{\lambda})^{-1}}{dl} = 3\pi e^2 [I_0(2) - I_1(2)] y^2, \quad (57b)$$

$$\frac{dy}{dl} = \left( 2 - \frac{\bar{K}}{8\pi} \right) y + 2\pi e I_0(2) y^2, \quad (57c)$$

first derived by Nelson and Halperin [2] and Young [3].

Following a standard analysis [1,2], the characteristic correlation length  $\xi_{\text{xtal-hex}}$  near the critical point at  $T \rightarrow T_m^-$  can be extracted from the above RG flows, and it is given by

$$\xi_{\text{xtal-hex}}(T) \sim a e^{-c/|T-T_m|^{\bar{\nu}}}, \quad (58)$$

with the hexagonal lattice exponent given by

$$\bar{\nu} = 0.3696 \dots, \quad (59)$$

and  $c$  is a nonuniversal constant [2].

## B. Hexatic-isotropic liquid transition

Dislocation-unbinding above the melting temperature  $T_m$  destroys the crystal order, restoring continuous translational symmetry. The plasma of unbound dislocations drives the shear modulus to zero, but it retains the quasi-long-ranged orientational order and the associated bond orientational stiffness. Inside this orientationally ordered hexatic fluid ( $T_m < T < T_{\text{hex}}$ ),  $g_b$  is driven to strong coupling, suppressing  $\mathbf{A}$  fluctuations, and allowing us to approximate the dislocation cosine by its harmonic form. With disclinations reinstated, the resulting effective Hamiltonian takes the standard scalar

sine-Gordon form:

$$\begin{aligned}\tilde{H}_{\text{hex}} &\approx \int_{\mathbf{r}} \left[ \frac{1}{2} g_b \sum_{n=1}^3 \epsilon_{ik} \epsilon_{jl} b_i^n b_j^n \partial_k \phi \partial_l \phi - g_s \cos \left( \frac{2\pi}{6} \phi \right) \right] \\ &= \int_{\mathbf{r}} \left[ \frac{1}{2} J (\nabla \phi)^2 - g_s \cos \left( \frac{2\pi}{6} \phi \right) \right],\end{aligned}\quad (60)$$

where  $J \equiv \frac{3}{2} a^2 g_b$ .

Alternatively, we can get to this dual hexatic Hamiltonian by noting that above the critical melting temperature,  $T_m$ , dislocations (disclination dipoles) unbind, leading to an orientationally ordered (a hexatic) fluid. Since the dislocations then appear at finite density, their Burgers charge  $\mathbf{b}(\mathbf{r})$  can be treated as a continuous (rather than a discrete) vector field. Going back to (27), carrying out a Gaussian integral over a continuous field  $\mathbf{b}_r$ , and summing over discrete disclination charges,  $s_{r_n}$ , we again obtain the hexatic Hamiltonian presented above.

Utilizing  $\tilde{H}_{\text{hex}}$ , we observe that within the hexatic phase, the energy of a disclination, screened by the plasma of proliferated dislocations, is reduced significantly from that of the crystal (where it diverges as  $L^2$ ) to  $E_s^{\text{hex}} \sim J_R \ln L/a$ . Thus, the hexatic-isotropic fluids transition is of the conventional Kosterlitz-Thouless type [1,2,17], taking place at  $T_{\text{hex}} = (72/\pi) J_R(T_{\text{hex}})$ . Above  $T_{\text{hex}}$ , the fluid is isotropic, characterized by short-ranged translational and orientational correlations.

#### IV. SUMMARY AND CONCLUSION

In this paper, starting with a description of a crystal in terms of its elasticity and topological defects, we derive a corresponding dual vector sine-Gordon model. In the latter, the disclinations and dislocations are captured by cosine operators of the Airy stress potential and its gradient. The relevance of the latter dislocation cosine signals the continuous Kosterlitz-Thouless-Halperin-Nelson-Young melting transition of a crystal into a hexatic fluid [1–3]. The subsequent relevance of the former disclination cosine captures the hexatic-to-isotropic fluid Kosterlitz-Thouless transition, as outlined in Sec. IB and illustrated in Fig. 1. Our complementary analysis reproduces straightforwardly the results of Nelson and Halperin [2] and Young [3], including the correlation functions, defect energetics, renormalization-group flows, and the correlation length exponent  $\bar{\nu}$ .

We expect that the simplified vector sine-Gordon formulation presented here will be useful in further detailed studies of, e.g., the external stress, the defect dynamics, the substrate, and the dynamics of the melting transition [25].

#### ACKNOWLEDGMENTS

We acknowledge useful discussions with Michael Pretko, and we thank him for valuable input on the manuscript. This work was supported by the Simons Investigator Award from

the James Simons Foundation and by NSF MRSEC Grant No. DMR-1420736. L.R. also thanks the KITP for its hospitality as part of the Fall 2016 Synthetic Matter workshop and sabbatical program, during which this work was initiated and supported by NSF Grant No. PHY-1125915.

#### APPENDIX A: DERIVATION OF RG EQUATIONS

In this Appendix, we present the details of the renormalization-group analysis of the vector sine-Gordon model for the dislocation unbinding transition,

$$\begin{aligned}\tilde{H} &= \int_{\mathbf{r}} \left[ \frac{1}{2} [K^{-1} (\partial_i A_j)^2 + B \partial_i A_j \partial_j A_i] + \frac{\alpha}{2} (\nabla \cdot \mathbf{A})^2 \right. \\ &\quad \left. - g_b \sum_{n=1}^3 \cos(\mathbf{b}_n \cdot \mathbf{A}) \right],\end{aligned}\quad (A1)$$

where the coupling constants are  $K^{-1} = \frac{2\mu+\lambda}{4\mu(\mu+\lambda)}$  and  $B = \frac{\lambda}{4\mu(\mu+\lambda)}$ . The transversality constraint  $\nabla \cdot \mathbf{A} = \mathbf{0}$  is imposed energetically by taking  $\alpha \rightarrow \infty$  at the end of the calculation.

In the physical limit  $\alpha \rightarrow \infty$ , the dislocation-free, Gaussian propagator is given by

$$\langle A_i(\mathbf{q}) A_j(\mathbf{q}') \rangle_0 = \frac{K}{q^2} P_{ij}^T(\mathbf{q}) (2\pi)^2 \delta^2(\mathbf{q} + \mathbf{q}'), \quad (A2)$$

with the transverse projection operator  $P_{ij}^T(\mathbf{q}) = \delta_{ij} - \frac{q_i q_j}{q^2}$ .

To carry out the momentum-shell RG analysis, we decompose vector field  $\mathbf{A}(\mathbf{r})$  into its short- and long-scale modes,  $A_i(\mathbf{r}) = A_i^<(\mathbf{r}) + A_i^>(\mathbf{r})$ , with

$$A_i^<(\mathbf{r}) = \int_{0 < q < \Lambda/b} \frac{d^2 q}{(2\pi)^2} e^{i\mathbf{q}\cdot\mathbf{r}} A_i(\mathbf{q}), \quad (A3a)$$

$$A_i^>(\mathbf{r}) = \int_{\Lambda/b < q < \Lambda} \frac{d^2 q}{(2\pi)^2} e^{i\mathbf{q}\cdot\mathbf{r}} A_i(\mathbf{q}), \quad (A3b)$$

where the ultraviolet cutoff  $\Lambda = 2\pi/a$ , and the rescaling factor  $b > 1$  defines the width of the momentum shell,  $\Lambda/b < q < \Lambda$ .

Integrating out the short-scale modes,  $A_i^>(\mathbf{r})$ , the partition function reduces to integration over the long-scale modes,  $A_i^<(\mathbf{r})$ , with an effective Hamiltonian,

$$\begin{aligned}Z &= \int [d\mathbf{A}] e^{-H[\mathbf{A}^> + \mathbf{A}^<]} \\ &= \int [d\mathbf{A}^<] [d\mathbf{A}^>] e^{-H_0[\mathbf{A}^<] - H_0[\mathbf{A}^>] - H_{\text{int}}[\mathbf{A}^< + \mathbf{A}^>]} \\ &= \int [d\mathbf{A}^<] e^{-H_0[\mathbf{A}^<]} Z_0^> \langle e^{-H_{\text{int}}[\mathbf{A}^< + \mathbf{A}^>]} \rangle_0 \equiv \int [d\mathbf{A}^<] e^{-H_{\text{eff}}[\mathbf{A}^<]},\end{aligned}\quad (A4)$$

where  $Z_0^> = \int [d\mathbf{A}^>] e^{-H_0[\mathbf{A}^>]}$  is the harmonic part of the partition function of the short-scale modes with the quadratic Hamiltonian,

$$H_0[\mathbf{A}^>] = \int_{\mathbf{r}} \left[ \frac{1}{2} [K^{-1} (\partial_i A_j^>)^2 + B \partial_i A_j^> \partial_j A_i^>] + \frac{\alpha}{2} (\nabla \cdot \mathbf{A}^>)^2 \right], \quad (A5)$$



and the coarse-grained effective Hamiltonian  $H_{<}[\mathbf{A}^<]$  of the long-scale modes given by

$$H_{<}[\mathbf{A}^<] = H_0[\mathbf{A}^<] - \ln \langle e^{-H_{\text{int}}[\mathbf{A}^< + \mathbf{A}^>]} \rangle_0 - \ln Z_0^>. \quad (\text{A6})$$

We drop the last term,  $-\ln Z_0^>$ , which is a field-independent correction to the free energy that does not affect the flow of the coupling constants. We then compute  $H_{<}[\mathbf{A}^<]$  in terms of corrections to elastic constants  $\mu$ ,  $\lambda$  and dislocation fugacity  $g_b$  arising from coarse-graining  $-\ln \langle e^{-H_{\text{int}}[\mathbf{A}^< + \mathbf{A}^>]} \rangle_0$ .

We expand  $\langle e^{-H_{\text{int}}[\mathbf{A}^< + \mathbf{A}^>]} \rangle_0$  to second order in  $g_b$ ,

$$\langle e^{-H_{\text{int}}[\mathbf{A}^< + \mathbf{A}^>]} \rangle_0 = \langle e^{g_b \sum_{n=1,2,3} \int_{\mathbf{r}} \cos(\mathbf{b}_n \cdot \mathbf{A})} \rangle_0 \approx 1 + g_b \sum_{n=1}^3 \int_{\mathbf{r}} \langle \cos(\mathbf{b}_n \cdot \mathbf{A}) \rangle_0 + \frac{g_b^2}{2} \sum_{n=1}^3 \sum_{m=1}^3 \int_{\mathbf{r}_1} \int_{\mathbf{r}_2} \langle \cos[\mathbf{b}_n \cdot \mathbf{A}(\mathbf{r}_1)] \cos[\mathbf{b}_m \cdot \mathbf{A}(\mathbf{r}_2)] \rangle_0, \quad (\text{A7})$$

finding

$$\begin{aligned} \ln \langle e^{-H_{\text{int}}[\mathbf{A}^< + \mathbf{A}^>]} \rangle_0 &= g_b \sum_{n=1}^3 \int_{\mathbf{r}} \langle \cos(\mathbf{b}_n \cdot \mathbf{A}) \rangle_0 + \frac{g_b^2}{2} \sum_{n,m=1}^3 \int_{\mathbf{r}_1} \int_{\mathbf{r}_2} \{ \langle \cos[\mathbf{b}_n \cdot \mathbf{A}(\mathbf{r}_1)] \cos[\mathbf{b}_m \cdot \mathbf{A}(\mathbf{r}_2)] \rangle_0 \\ &\quad - \langle \cos[\mathbf{b}_n \cdot \mathbf{A}(\mathbf{r}_1)] \rangle_0 \langle \cos[\mathbf{b}_m \cdot \mathbf{A}(\mathbf{r}_2)] \rangle_0 \}. \end{aligned} \quad (\text{A8})$$

These are straightforwardly evaluated by Gaussian integration, giving to first order

$$\langle \cos(\mathbf{b}_n \cdot \mathbf{A}) \rangle_0 = \frac{1}{2} \langle e^{i\mathbf{b}_n \cdot (\mathbf{A}^< + \mathbf{A}^>)} + e^{-i\mathbf{b}_n \cdot (\mathbf{A}^< + \mathbf{A}^>)} \rangle_0 = e^{-\frac{1}{2} \langle (\mathbf{b}_n \cdot \mathbf{A}^>)^2 \rangle_0} \cos(\mathbf{b}_n \cdot \mathbf{A}^<) \equiv e^{-\frac{1}{2} G_{nm}^>(0)} \cos(\mathbf{b}_n \cdot \mathbf{A}^<), \quad (\text{A9})$$

and to second order the connected part,

$$\begin{aligned} &\langle \cos[\mathbf{b}_n \cdot \mathbf{A}(\mathbf{r}_1)] \cos[\mathbf{b}_m \cdot \mathbf{A}(\mathbf{r}_2)] \rangle_0 - \langle \cos[\mathbf{b}_n \cdot \mathbf{A}(\mathbf{r}_1)] \rangle_0 \langle \cos[\mathbf{b}_m \cdot \mathbf{A}(\mathbf{r}_2)] \rangle_0 \\ &= \frac{1}{4} \{ e^{i[\mathbf{b}_n \cdot \mathbf{A}^<(\mathbf{r}_1) + \mathbf{b}_m \cdot \mathbf{A}^<(\mathbf{r}_2)]} \langle e^{i[\mathbf{b}_n \cdot \mathbf{A}^>(\mathbf{r}_1) + \mathbf{b}_m \cdot \mathbf{A}^>(\mathbf{r}_2)]} \rangle_0 + e^{i[\mathbf{b}_n \cdot \mathbf{A}^<(\mathbf{r}_1) - \mathbf{b}_m \cdot \mathbf{A}^<(\mathbf{r}_2)]} \langle e^{i[\mathbf{b}_n \cdot \mathbf{A}^>(\mathbf{r}_1) - \mathbf{b}_m \cdot \mathbf{A}^>(\mathbf{r}_2)]} \rangle_0 \\ &\quad + e^{-i[\mathbf{b}_n \cdot \mathbf{A}^<(\mathbf{r}_1) - \mathbf{b}_m \cdot \mathbf{A}^<(\mathbf{r}_2)]} \langle e^{-i[\mathbf{b}_n \cdot \mathbf{A}^>(\mathbf{r}_1) - \mathbf{b}_m \cdot \mathbf{A}^>(\mathbf{r}_2)]} \rangle_0 + e^{-i[\mathbf{b}_n \cdot \mathbf{A}^<(\mathbf{r}_1) + \mathbf{b}_m \cdot \mathbf{A}^<(\mathbf{r}_2)]} \langle e^{-i[\mathbf{b}_n \cdot \mathbf{A}^>(\mathbf{r}_1) + \mathbf{b}_m \cdot \mathbf{A}^>(\mathbf{r}_2)]} \rangle_0 \} \\ &\quad - e^{-G_{nm}^>(0)} \cos[\mathbf{b}_n \cdot \mathbf{A}^<(\mathbf{r}_1)] \cos[\mathbf{b}_m \cdot \mathbf{A}^<(\mathbf{r}_2)] \\ &= \frac{1}{2} e^{-G_{nm}^>(0)} \{ [e^{-G_{nm}^>(v)} - 1] \cos[\mathbf{b}_n \cdot \mathbf{A}^<(\mathbf{r}_1) + \mathbf{b}_m \cdot \mathbf{A}^<(\mathbf{r}_2)] + [e^{+G_{nm}^>(v)} - 1] \cos[\mathbf{b}_n \cdot \mathbf{A}^<(\mathbf{r}_1) - \mathbf{b}_m \cdot \mathbf{A}^<(\mathbf{r}_2)] \}, \end{aligned} \quad (\text{A10})$$

where  $\mathbf{v} = \mathbf{r}_1 - \mathbf{r}_2$ , and we have defined

$$G_{nm}^>(\mathbf{r}_1 - \mathbf{r}_2) \equiv b_i^n b_j^m \langle A_i^>(\mathbf{r}_1) A_j^>(\mathbf{r}_2) \rangle_0. \quad (\text{A11})$$

For  $0 < v < a$ , we approximate the short-scale averaged correlation function by its value at  $v = 0$ ,

$$\langle A_i^>(\mathbf{r}) A_j^>(\mathbf{r}) \rangle_0 = \int_{\mathbf{q}} \langle A_i(\mathbf{q}) A_j(-\mathbf{q}) \rangle_0 = \int_{\Lambda/b}^{\Lambda} \frac{qdq}{(2\pi)^2} \int_0^{2\pi} d\theta \frac{K}{q^2} \left( \delta_{ij} - \frac{q_i q_j}{q^2} \right) = \frac{K}{2\pi} \ln b \left( \delta_{ij} - \frac{1}{2} \delta_{ij} \right) = \frac{K}{4\pi} \ln b \delta_{ij}. \quad (\text{A12})$$

For  $v > a$ , we have the real space correlation function [2],

$$\langle A_i(\mathbf{r}_1) A_j(\mathbf{r}_2) \rangle = \int \frac{d^2q}{(2\pi)^2} \langle A_i(\mathbf{q}) A_j(-\mathbf{q}) \rangle \cdot e^{i\mathbf{q} \cdot (\mathbf{r}_1 - \mathbf{r}_2)} = \int \frac{d^2q}{(2\pi)^2} \frac{K}{q^2} \left( \delta_{ij} - \frac{q_i q_j}{q^2} \right) \cdot e^{i\mathbf{q} \cdot \mathbf{v}} = -\frac{K}{4\pi} \left( \ln \frac{v}{a} \delta_{ij} - \frac{v_i v_j}{v^2} \right). \quad (\text{A13})$$

Therefore, we can evaluate  $G_{nm}^>(\mathbf{r}_1 - \mathbf{r}_2)$  explicitly, finding

$$G_{nm}^>(\mathbf{r}_1 - \mathbf{r}_2) \approx \begin{cases} \frac{K}{4\pi} \mathbf{b}_n \cdot \mathbf{b}_m \ln b \text{ for } 0 < v < a, \\ -\frac{K}{4\pi} \left[ \mathbf{b}_n \cdot \mathbf{b}_m \ln \frac{v}{ba} - \frac{(\mathbf{b}_n \cdot \mathbf{v})(\mathbf{b}_m \cdot \mathbf{v})}{v^2} \right] \text{ for } a < v < ba, \\ 0 \text{ for } v > ba. \end{cases} \quad (\text{A14})$$

This thus gives to second-order in  $g_b$ ,

$$\begin{aligned} \ln \langle e^{-H_{\text{int}}[\mathbf{A}^< + \mathbf{A}^>]} \rangle_0 &= g_b \sum_n \int_{\mathbf{r}} e^{-\frac{1}{2} G_{nm}^>(0)} \cos(\mathbf{b}_n \cdot \mathbf{A}^<) + \frac{g_b^2}{4} \sum_{n,m} e^{-G_{nm}^>(0)} \left\{ \int_{\mathbf{r}_1} \int_{\mathbf{r}_2} [e^{-G_{nm}^>(\mathbf{r}_1 - \mathbf{r}_2)} - 1] \right. \\ &\quad \times \cos[\mathbf{b}_n \cdot \mathbf{A}^<(\mathbf{r}_1) + \mathbf{b}_m \cdot \mathbf{A}^<(\mathbf{r}_2)] + \int_{\mathbf{r}_1} \int_{\mathbf{r}_2} [e^{+G_{nm}^>(\mathbf{r}_1 - \mathbf{r}_2)} - 1] \times \cos[\mathbf{b}_n \cdot \mathbf{A}^<(\mathbf{r}_1) - \mathbf{b}_m \cdot \mathbf{A}^<(\mathbf{r}_2)] \left. \right\}. \end{aligned} \quad (\text{A15})$$

The above double integral,  $\int d^2r_1 \int d^2r_2 (\dots)$  simplifies using the fact that  $G_{nm}^>(\mathbf{r}_1 - \mathbf{r}_2)$  is short-ranged, vanishing for  $|\mathbf{r}_1 - \mathbf{r}_2|$  larger than  $b/\Lambda \sim ba$ , since  $G_{nm}^>(\mathbf{r})$  is defined to be composed of Fourier modes only within a thin momentum-shell,

$\Lambda/b < q < \Lambda$ . Consequently,  $[e^{\pm G_{nm}^>(\mathbf{r}_1-\mathbf{r}_2)} - 1]$  is also small everywhere but in the range  $|\mathbf{r}_1 - \mathbf{r}_2| \sim b/\Lambda \sim ba$ . To utilize these observations, we change variables  $\{\mathbf{r}_1, \mathbf{r}_2\}$  to their sum and difference,

$$\mathbf{r} = \frac{1}{2}(\mathbf{r}_1 + \mathbf{r}_2), \quad \mathbf{v} = \mathbf{r}_1 - \mathbf{r}_2, \quad (\text{A16})$$

obtaining

$$\mathbf{b}_n \cdot \mathbf{A}^<(\mathbf{r}_1) + \mathbf{b}_m \cdot \mathbf{A}^<(\mathbf{r}_2) \approx (\mathbf{b}_n + \mathbf{b}_m) \cdot \mathbf{A}^<(\mathbf{r}) \quad (\text{A17})$$

and

$$\mathbf{b}_n \cdot \mathbf{A}^<(\mathbf{r}_1) - \mathbf{b}_m \cdot \mathbf{A}^<(\mathbf{r}_2) = \mathbf{b}_n \cdot \mathbf{A}^<\left(\mathbf{r} + \frac{\mathbf{v}}{2}\right) - \mathbf{b}_m \cdot \mathbf{A}^<\left(\mathbf{r} - \frac{\mathbf{v}}{2}\right) \approx (\mathbf{b}_n - \mathbf{b}_m) \cdot \mathbf{A}^<(\mathbf{r}) + \frac{1}{2}(\mathbf{b}_n + \mathbf{b}_m) \cdot (\mathbf{v} \cdot \nabla) \mathbf{A}^<(\mathbf{r}). \quad (\text{A18})$$

This allows the following simplifications of (A15),

$$\begin{aligned} \ln \langle e^{-H_{\text{int}}[\mathbf{A}^<+\mathbf{A}^>]} \rangle_0^> &\approx g_b \sum_n e^{-\frac{1}{2}G_{nm}^>(0)} \int_{\mathbf{r}} \cos(\mathbf{b}_n \cdot \mathbf{A}^<) + \frac{g_b^2}{4} \sum_{n,m} e^{-G_{nm}^>(0)} \left\{ \int_{\mathbf{r}} \int_{\mathbf{v}} [e^{-G_{nm}^>(\mathbf{v})} - 1] \cos[(\mathbf{b}_n + \mathbf{b}_m) \cdot \mathbf{A}^<(\mathbf{r})] \right. \\ &\quad \left. + [e^{+G_{nm}^>(\mathbf{v})} - 1] \cos \left[ \left( (\mathbf{b}_n - \mathbf{b}_m) + \frac{1}{2}(\mathbf{b}_n + \mathbf{b}_m)(\mathbf{v} \cdot \nabla) \right) \cdot \mathbf{A}^<(\mathbf{r}) \right] \right\}. \end{aligned} \quad (\text{A19})$$

Comparing (A19) to the component of the long-scale Hamiltonian  $H[\mathbf{A}^<]$ , we can extract the corresponding corrections for the coupling constants  $K^{-1}$ ,  $B$ , and  $g_b$ . To this end, ignoring the field-independent terms, we obtain

$$\begin{aligned} \ln \langle e^{-H_{\text{int}}[\mathbf{A}^<+\mathbf{A}^>]} \rangle_0^> &\approx g_b \sum_n e^{-\frac{1}{2}G^>(0)} \int_{\mathbf{r}} \cos(\mathbf{b}_n \cdot \mathbf{A}^<) + \frac{g_b^2}{4} \sum_{n,m} e^{-G^>(0)} \left\{ \int_{\mathbf{r}} \int_{\mathbf{v}} [e^{-G_{nm}^>(\mathbf{v})} - 1] \cos[(\mathbf{b}_n + \mathbf{b}_m) \cdot \mathbf{A}^<(\mathbf{r})] \right. \\ &\quad \left. + \int_{\mathbf{r}} \int_{\mathbf{v}} [e^{+G_{nm}^>(\mathbf{v})} - 1] \left[ \cos[(\mathbf{b}_n - \mathbf{b}_m) \cdot \mathbf{A}^<] - \frac{1}{8} [(\mathbf{b}_n + \mathbf{b}_m) \cdot (\mathbf{v} \cdot \nabla) \mathbf{A}^<]^2 \cos[(\mathbf{b}_n - \mathbf{b}_m) \cdot \mathbf{A}^<] \right] \right\} \\ &= g_b \sum_n e^{-\frac{1}{2}G^>(0)} \int_{\mathbf{r}} \cos(\mathbf{b}_n \cdot \mathbf{A}^<) + g_b^2 \int_{\mathbf{r}} \{ I_{23} \cos[\mathbf{b}_1 \cdot \mathbf{A}^<(\mathbf{r})] + I_{13} \cos[\mathbf{b}_2 \cdot \mathbf{A}^<(\mathbf{r})] + I_{12} \cos[\mathbf{b}_3 \cdot \mathbf{A}^<(\mathbf{r})] \} \\ &\quad - \frac{g_b^2}{8} \sum_n e^{-G^>(0)} \int_{\mathbf{r}} \int_{\mathbf{v}} [e^{+G_{nm}^>(\mathbf{v})} - 1] [\mathbf{b}_n \cdot (\mathbf{v} \cdot \nabla) \mathbf{A}^<]^2 + \text{other irrelevant terms}. \end{aligned} \quad (\text{A20})$$

We note that above, we have written  $G_{nm}^>(0)$  simply as  $G^>(0)$ , since it takes the same value for all elementary Burgers vectors  $\mathbf{b}_n$ ,  $n = 1, 2, 3$ . Further simplifications lead to the desired form

$$\ln \langle e^{-H_{\text{int}}[\mathbf{A}^<+\mathbf{A}^>]} \rangle_0^> \approx \int_{\mathbf{r}} \left\{ \sum_n [g_b e^{-\frac{1}{2}G^>(0)} + J_1 g_b^2] \cos(\mathbf{b}_n \cdot \mathbf{A}^<) - \frac{g_b^2}{2} [J_2 (\partial_i A_j^<)^2 + J_3 \partial_i A_j^< \partial_j A_i^< + J_3 (\nabla \cdot \mathbf{A}^<)^2] \right\}, \quad (\text{A21})$$

where the coefficients  $J_1$ ,  $J_2$ , and  $J_3$  are defined as

$$J_1 = I_{12} = I_{13} = I_{23} \equiv \frac{1}{2} e^{-G^>(0)} \int_{\mathbf{v}} [e^{-G_{12}^>(\mathbf{v})} - 1] = \pi a^2 \left[ e^{\frac{\bar{K}}{16\pi}} I_0\left(\frac{\bar{K}}{8\pi}\right) + \left(\frac{\bar{K}}{16\pi} - 1\right) \right] \delta l, \quad (\text{A22a})$$

$$J_2 = \frac{1}{4} \sum_{n=1}^3 (b_2^n)^2 e^{-G^>(0)} \int_{\mathbf{v}} v_1^2 [e^{+G_{nm}^>(\mathbf{v})} - 1] = \frac{\pi a^6}{4} \left\{ e^{\frac{\bar{K}}{8\pi}} \left[ \frac{3}{2} I_0\left(\frac{\bar{K}}{8\pi}\right) - \frac{3}{4} I_1\left(\frac{\bar{K}}{8\pi}\right) \right] + \frac{3}{2} \left(\frac{\bar{K}}{16\pi} - 1\right) \right\} \delta l, \quad (\text{A22b})$$

$$J_3 = \frac{1}{4} e^{-G^>(0)} \sum_n b_1^n b_2^n \int_{\mathbf{v}} v_1 v_2 (e^{+G_{nm}^>(\mathbf{v})} - 1) = \frac{3\pi a^6}{16} e^{\frac{\bar{K}}{8\pi}} I_1\left(\frac{\bar{K}}{8\pi}\right) \delta l. \quad (\text{A22c})$$

Above  $I_0(x)$ ,  $I_1(x)$  are modified Bessel functions, we have dropped higher harmonic operators, and we have taken  $\delta l \equiv \ln b \ll 1$ .

The above analysis now allows us to identify the renormalized couplings  $K_R^{-1}$ ,  $B_R$ , and  $g_{b_R}$ ,

$$K_R^{-1}(b) = K^{-1} + J_2 g_b^2, \quad (\text{A23a})$$

$$B_R(b) = B + J_3 g_b^2, \quad (\text{A23b})$$

$$g_{b_R}(b) = g_b e^{-\frac{1}{2}G^>(0)} + J_1 g_b^2, \quad (\text{A23c})$$

obtained to second-order in  $g_b$ . The corresponding RG differential flow equations for the dimensionless couplings  $\bar{K}^{-1}(l) = K^{-1}/a^2$ ,  $\bar{B}(l) = B/a^2$ ,  $\bar{g}_b(l) = g_b a^2$  are then given by

$$\frac{d\bar{K}^{-1}(l)}{dl} = \frac{3\pi}{8} \left\{ e^{\frac{\bar{K}}{8\pi}} \left[ I_0\left(\frac{\bar{K}}{8\pi}\right) - \frac{1}{2} I_1\left(\frac{\bar{K}}{8\pi}\right) \right] + \frac{\bar{K}}{16\pi} - 1 \right\} \bar{g}_b^2, \quad (\text{A24a})$$

$$\frac{d\bar{B}(l)}{dl} = \frac{3\pi}{16} e^{\frac{\bar{K}}{8\pi}} I_1\left(\frac{\bar{K}}{8\pi}\right) \bar{g}_b^2, \quad (\text{A24b})$$

$$\frac{d\bar{g}_b(l)}{dl} = \left( 2 - \frac{\bar{K}}{8\pi} \right) \bar{g}_b + \pi \left[ e^{\frac{\bar{K}}{16\pi}} I_0\left(\frac{\bar{K}}{8\pi}\right) + \left( \frac{\bar{K}}{16\pi} - 1 \right) \right] \bar{g}_b^2. \quad (\text{A24c})$$

Near the melting critical point,  $\bar{K}^{-1}(l \rightarrow \infty) = \frac{1}{16\pi}$ ,  $\bar{g}_b(l \rightarrow \infty) = 0$ , we define the reduced temperature,  $x(l) = \frac{16\pi}{\bar{K}} - 1$ , and fugacity,  $y(l) = e^{-E_{cs}} = \frac{1}{2} \bar{g}_b$ . Near the melting point, their flow equations are given by

$$\frac{dx(l)}{dl} = 12\pi^2 e^2 [2I_0(2) - I_1(2)] y^2 \equiv 12\pi^2 c_1 y^2, \quad (\text{A25a})$$

$$\frac{dy(l)}{dl} = 2xy + 2\pi e I_0(2) y^2 \equiv 2xy + 2\pi c_2 y^2, \quad (\text{A25b})$$

where  $c_1 = e^2 [2I_0(2) - I_1(2)] = 21.937 \dots$  and  $c_2 = e I_0(2) = 6.1965 \dots$  are numerical constants, consistent with Halperin and Nelson [2].

Following a standard analysis [1,2], the characteristic correlation length  $\xi_{\text{xtal-hex}}$  near the critical point at  $T \rightarrow T_m^-$  can be extracted from the above RG flows, giving

$$\xi_{\text{xtal-hex}}(T) \sim a e^{-c/|T-T_m|^\bar{\nu}}, \quad (\text{A26})$$

with the hexagonal lattice exponent given by  $\bar{\nu} = 0.3696 \dots$  and  $c$  is a nonuniversal constant.

Using the expressions of  $K$  and  $B$  in terms of the dimensionless Lamé elastic constants  $\bar{\mu} = \mu a^2$  and  $\bar{\lambda} = \lambda a^2$ ,

$$\bar{K}^{-1} = \frac{1}{4} \left( \frac{1}{\bar{\mu}} + \frac{1}{\bar{\mu} + \bar{\lambda}} \right), \quad (\text{A27a})$$

$$\bar{B} = \frac{1}{4} \left( \frac{1}{\bar{\mu}} - \frac{1}{\bar{\mu} + \bar{\lambda}} \right), \quad (\text{A27b})$$

the RG flow equations for the inverse shear modulus,  $\mu^{-1}(l)$ , and the inverse bulk modulus,  $[\mu(l) + \lambda(l)]^{-1}$ , near the critical point are then given by

$$\frac{d\bar{\mu}^{-1}(l)}{dl} = 3\pi e^2 I_0(2) y^2(l), \quad (\text{A28a})$$

$$\frac{d[\bar{\mu}(l) + \bar{\lambda}(l)]^{-1}}{dl} = 3\pi e^2 [I_0(2) - I_1(2)] y^2(l). \quad (\text{A28b})$$

## APPENDIX B: ELASTICITY OF 2D CRYSTAL SUBJECT TO AN EXTERNAL STRESS FIELD

As the crystal is subject to an external stress tensor field  $\sigma_{ij}^e(\mathbf{r})$ , we need to add an external term into the elastic energy functional

$$\mathcal{H} = \frac{1}{2} C_{ij,kl} u_{ij} u_{kl} - \sigma_{ij}^e u_{ij}. \quad (\text{B1})$$

In the presence of topological defects, the distortion field  $\mathbf{u}(\mathbf{r})$  is not single-valued. It and the associated strain tensor

can be decomposed into the single-valued elastic phonon and the singular part,

$$u_i = \tilde{u}_i + u_i^s, \quad (\text{B2})$$

$$u_{ij} = \tilde{u}_{ij} + u_{ij}^s. \quad (\text{B3})$$

To include these topological and phonon degrees of freedom, we focus on the partition function (taking  $k_B T = 1$ , i.e., measuring coupling constants in units of thermal energy),

$$Z = \int [d\mathbf{u}] e^{-\int_r \mathcal{H}[\mathbf{u}]} = \int [d\mathbf{u}] \int [d\sigma_{ij}] e^{-\int_r \mathcal{H}[\mathbf{u}, \sigma_{ij}]}, \quad (\text{B4})$$

where the trace over  $\mathbf{u}(\mathbf{r})$  in the partition function (as in summing/integrating over the degrees of freedom of the theory) implicitly includes both phonons and topological defects by allowing non-single-valued distortions. In the second form, above, we decoupled the elastic energy by introducing a Hubbard-Stratonovich tensor field—the *symmetric* stress tensor  $\sigma_{ij}(\mathbf{r})$  with the resulting Hamiltonian density given by

$$\begin{aligned} \mathcal{H}[\mathbf{u}, \sigma_{ij}] &= \frac{1}{2} C_{ij,kl}^{-1} \sigma_{ij} \sigma_{kl} + i \sigma_{ij} u_{ij} - \sigma_{ij}^e u_{ij} \\ &= \frac{1}{2} C_{ij,kl}^{-1} \sigma_{ij} \sigma_{kl} + i (\sigma_{ij} + i \sigma_{ij}^e) (\partial_i \tilde{u}_j + u_{ij}^s), \end{aligned} \quad (\text{B5})$$

and  $C_{ij,kl}^{-1} = -\frac{\lambda}{4\mu(\mu+\lambda)} \delta_{ij} \delta_{kl} + \frac{1}{2\mu} \delta_{ik} \delta_{jl}$  for a 2D hexagonal lattice.

Tracing over the single-valued phonons  $\tilde{\mathbf{u}}$  enforces the divergenceless stress constraint,

$$\partial_i (\sigma_{ij} + i \sigma_{ij}^e) = 0, \quad (\text{B6})$$

solved with a scalar Airy stress potential,  $\phi(\mathbf{r})$ ,

$$\sigma_{ij} = \epsilon_{ik} \epsilon_{jl} \partial_k \partial_l \phi - i \sigma_{ij}^e. \quad (\text{B7})$$

Expressing the Hamiltonian density in terms of  $\phi(\mathbf{r})$ , and integrating by parts in the second linear term, we utilize the defects conditions, Eqs. (9) and (11),

$$\epsilon_{ik} \epsilon_{jl} \partial_l \partial_k u_{ij}^s = \epsilon_{ik} \epsilon_{jl} \partial_l \partial_k (\partial_i u_j^s - \epsilon_{ij} \theta^s), \quad (\text{B8a})$$

$$= \epsilon_{ki} \partial_k b_i(\mathbf{r}) + \epsilon_{ki} \partial_k \partial_i \theta(\mathbf{r}), \quad (\text{B8b})$$

$$= \hat{\mathbf{z}} \cdot \nabla \times \mathbf{b} + \frac{2\pi}{6} s(\mathbf{r}), \quad (\text{B8c})$$

to obtain

$$\begin{aligned} \mathcal{H}[\phi] &= \frac{1}{2} \tilde{C}_{ij,kl}^{-1} (\partial_i \partial_j \phi - i \epsilon_{ia} \epsilon_{jb} \sigma_{ij}^e) (\partial_k \partial_l \phi - i \epsilon_{kc} \epsilon_{ld} \sigma_{kl}^e) \\ &\quad + i \frac{1}{2} \epsilon_{ik} \epsilon_{jl} \partial_k \partial_l \phi (\partial_i u_j^s + \partial_j u_i^s) \end{aligned}$$

$$\begin{aligned}
&= \frac{1}{2}\tilde{C}_{ij,kl}^{-1}\partial_i\partial_j\phi\partial_k\partial_l\phi + i\frac{1}{2}\epsilon_{ik}\epsilon_{jl}\partial_k\partial_l\phi(\partial_i u_j^s - \partial_j u_i^s) \\
&\quad + i\epsilon_{ik}\epsilon_{jl}\partial_k\partial_l\phi\partial_j u_i^s - \frac{1}{2}C_{ij,kl}^{-1}\sigma_{ij}^e\sigma_{kl}^e - i\tilde{C}_{ij,kl}^{-1}\partial_i\partial_j\phi\sigma_{kl}^e \\
&= \frac{1}{2}\tilde{C}_{ij,kl}^{-1}\partial_i\partial_j\phi\partial_k\partial_l\phi + i\phi(2\pi s + \hat{\mathbf{z}} \cdot \nabla \times \mathbf{b}) \\
&\quad - \frac{1}{2}C_{ij,kl}^{-1}\sigma_{ij}^e\sigma_{kl}^e - i\tilde{C}_{ij,kl}^{-1}\partial_i\partial_j\phi\sigma_{kl}^e \\
&\equiv \mathcal{H}^{\text{int}}[\phi] + \mathcal{H}^{\text{ext}}[\phi], \tag{B9}
\end{aligned}$$

where  $\tilde{C}_{ij,kl} = \epsilon_{ia}\epsilon_{jb}\epsilon_{kc}\epsilon_{ld}C_{ab,cd}$ ,  $\tilde{\tilde{C}}_{ij,kl} = \epsilon_{ia}\epsilon_{jb}C_{ab,kl}$ , and we have used integration by parts. The total elastic energy functional is therefore composed of an internal part and an external part, with the internal part

$$\begin{aligned}
\mathcal{H}^{\text{int}} &= \frac{1}{2}\tilde{C}_{ij,kl}^{-1}\partial_i\partial_j\phi\partial_k\partial_l\phi + i\phi(2\pi s + \hat{\mathbf{z}} \cdot \nabla \times \mathbf{b}) \\
&\quad + E_{c_s}s^2 + E_{c_b}b^2, \tag{B10}
\end{aligned}$$

where we have added the dislocation and disclination core energies  $E_{cb}$  and  $E_{cs}$  to account for their short-scales, and the external part

$$\mathcal{H}^{\text{ext}} = -\frac{1}{2}C_{ij,kl}^{-1}\sigma_{ij}^e\sigma_{kl}^e - i\tilde{C}_{ij,kl}^{-1}\partial_i\partial_j\phi\sigma_{kl}^e. \tag{B11}$$

Alternatively, we can also start by formulating the elastic energy in terms of both the full strain tensor  $\partial_i u_j$  and the bond angle  $\theta(\mathbf{r})$ ,

$$\begin{aligned}
\mathcal{H} &= \frac{1}{2}C_{ij,kl}(\partial_i u_j - \theta\epsilon_{ij})(\partial_k u_l - \theta\epsilon_{kl}) + \frac{1}{2}K(\partial_i\theta)^2 \\
&\quad - \sigma_{ij}^e(\partial_i u_j - \theta\epsilon_{ij}), \tag{B12}
\end{aligned}$$

and we get the same result following the procedure of Sec. II C.

- 
- [1] J. M. Kosterlitz and D. J. Thouless, *J. Phys. C* **6**, 1181 (1972).  
[2] D. R. Nelson and B. I. Halperin, *Phys. Rev. B* **19**, 2457 (1979).  
[3] A. P. Young, *Phys. Rev. B* **19**, 1855 (1979).  
[4] L. D. Landau, *Phys. Z. Sowjetunion* **II**, 26 (1937).  
[5] R. E. Peierls, *Ann. Inst. Henri Poincaré* **5**, 177 (1935).  
[6] V. L. Berezinskii, *Zh. Eksp. Teor. Fiz.* **59**, 907 (1970) [*Sov. Phys. JETP* **32**, 493 (1971)].  
[7] V. L. Berezinskii, *Zh. Eksp. Teor. Fiz.* **61**, 1144 (1972) [*Sov. Phys. JETP* **34**, 601 (1972)].  
[8] B. I. Halperin, in *Proceeding of Kyoto Summer Institute 1979-Physics of Low Dimensional Systems*, edited by Y. Nagaoka and S. Hikami (Publications Office, Progress of Theoretical Physics, Kyoto, 1979).  
[9] D. R. Nelson, in *Phase transitions and Critical Phenomena*, edited by C. Domb and J. L. Lebowitz, Vol. 7 (Academic, New York, 1983).  
[10] C. C. Huang and T. Stoebe, *Adv. Phys.* **42**, 343 (1993).  
[11] C. M. Knobler, *Adv. Chem. Phys.* **77**, 397 (2007).  
[12] C. A. Murray and D. H. Van Winkle, *Phys. Rev. Lett.* **58**, 1200 (1987).  
[13] K. Zahn, R. Lenke, and G. Maret, *Phys. Rev. Lett.* **82**, 2721 (1999).  
[14] D. J. Amit, Y. Y. Goldschmidt, and G. Grinstein, *J. Phys. A* **13**, 585 (1980).  
[15] J. V. José, L. P. Kadanoff, S. Kirkpatrick, and D. R. Nelson, *Phys. Rev. B* **16**, 1217 (1977).  
[16] L. Benfatto, C. Castellani, and T. Giamarchi, *Phys. Rev. Lett.* **99**, 207002 (2007).  
[17] P. M. Chaikin and T. C. Lubensky, *Principles of Condensed Matter Physics* (Cambridge University Press, Cambridge, 1995).  
[18] L. Radzihovsky and T. C. Lubensky, *Phys. Rev. E* **83**, 051701 (2011).  
[19] T. Senthil, D. T. Son, C. Wang, and C. Xu, [arXiv:1810.05174](https://arxiv.org/abs/1810.05174).  
[20] M. Pretko and L. Radzihovsky, *Phys. Rev. Lett.* **120**, 195301 (2018).  
[21] M. Pretko and L. Radzihovsky, *Phys. Rev. Lett.* **121**, 235301 (2018).  
[22] R. M. Nandkishore and M. Hermele, *Annu. Rev. Condens. Matter Phys.* **10**, 295 (2019).  
[23] T. Ohta, *Prog. Theor. Phys.* **63**, 785 (1980).  
[24] Y. Levin and K. A. Dawson, *Phys. Rev. A* **42**, 3507 (1990); Y. Levin, *Phys. Rev. B* **43**, 10876 (1991).  
[25] A. Zippelius, B. I. Halperin, and D. R. Nelson, *Phys. Rev. B* **22**, 2514 (1980).